Available online at www.sciencedirect.com
ScienceDirect
International Journal of Multiphase Flow 33 (2007) 1284–1295
International Journal of Multiphase Flow
www.elsevier.com/locate/ijmulflow

Boiling heat transfer characteristics of nanofluids in a flat heat pipe evaporator with micro-grooved heating surface

Zhen-hua Liu *, Jian-guo Xiong, Ran Bao

School of Mechanical and Power Engineering, Shanghai Jiaotong University, Shanghai 200030, PR China

Received 11 February 2007; received in revised form 30 May 2007

Abstract

An experimental study was performed to understand the nucleate boiling heat transfer of water–CuO nanoparticles suspension (nanofluids) at different operating pressures and different nanoparticle mass concentrations. The experimental apparatus is a miniature flat heat pipe (MFHP) with micro-grooved heat transfer surface of its evaporator. The experimental results indicate that the operating pressure has great influence on the nucleate boiling characteristics in the MFHP evaporator. The heat transfer coefficient and the critical heat flux (CHF) of nanofluids increase greatly with decreasing pressure as compared with those of water. The heat transfer coefficient and the CHF of nanofluids can increase about 25% and 50%, respectively, at atmospheric pressure whereas about 100% and 150%, respectively, at the pressure of 7.4 kPa. Nanoparticle mass concentration also has significant influence on the boiling heat transfer and the CHF of nanofluids. The heat transfer coefficient and the CHF increase slowly with the increase of the nanoparticle mass concentration at low concentration conditions. However, when the nanoparticle mass concentration is over 1.0 wt%, the CHF enhancement is close to a constant number and the heat transfer coefficient deteriorates. There exists an optimum mass concentration for nanofluids which corresponds to the maximum heat transfer enhancement and this optimum mass concentration is 1.0 wt% at all test pressures. The experiment confirmed that the boiling heat transfer characteristics of the MFHP evaporator can evidently be strengthened by using water/CuO nanofluids.

Keywords: Nanofluid; Boiling; CHF; Flat heat pipe; Micro-groove

1. Introduction

Nanofluid (nanoparticle-suspension), as a new kind of functional fluid, has many unique characteristics. It is an innovative research to use nanofluid technology in traditional thermal engineering fields. Stable nanofluids are produced by dispersing pure metallic nanoparticles, ceramic nanoparticles or carbon nanoparticles into base fluids such as water and ethylene glycol. So far, the studies on nanofluids mainly focused on the effective thermal conductivity (Lee et al., 1999; Eastman et al., 2001; Wang et al., 2003; Das et al., 2003a; Wen and

* Corresponding author. Tel.: +86 21 62932992; fax: +86 21 62933086.
E-mail address: liuzhenh@sjtu.edu.cn (Z.-h. Liu).

0301-9322/$ - see front matter © 2007 Elsevier Ltd. All rights reserved.
doi:10.1016/j.ijmultiphaseflow.2007.06.009

Ding, 2004) and the single phase convective heat transfer of nanofluids flowing in tubes (Xuan and Li, 2003; Maiga et al., 2004).

In recent years, some studies on phase-changing heat transfer of nanofluids have been reported. However these studies are limited and mainly focused on pool boiling heat transfer at atmospheric pressure (Das et al., 2003b; You et al., 2003; Vassallo et al., 2004; Bang and Chang, 2005; Wen and Ding, 2005).

Das et al. (2003b) conducted an investigation on the pool boiling of water–Al_2O_3 nanoparticles-suspension on a horizontal tubular heater having a diameter of 20 mm with different surface roughness at atmospheric pressure. No surfactant was added into suspensions. It was found that the boiling heat transfer of nanoparticle-suspensions was deteriorated compared to that of pure water. The wall superheat for nanofluids increased by about 30–130% when substituting nanofluids with the volume concentration of 4 wt% for pure water. Compared with pure water, surface roughness of the heating surface could also greatly affect the nucleation superheat. The required superheat for a smooth surface was higher than that for a rough surface. The subsidence of nanoparticles was considered as the main reason for the increase of the superheat.

Vassallo et al. (2004) carried out a pool experiment of silica–water nanoparticles-suspensions on a horizontal NiCr wire at atmospheric pressure. No surfactant was added into suspensions. The CHF has been enhanced 32% for horizontal flat surface and 13% for vertical flat surface in the pool. But, no appreciable differences in the boiling heat transfer were found for the heat flux less than the CHF.

Bang and Chang (2005) conducted an experimental investigation on the pool boiling of water–Al_2O_3 nanoparticles-suspensions on a plain plate at atmospheric pressure. As the cases of the two studies mentioned above, no surfactant was added into suspensions in their experiment. It was found that the boiling heat transfer characteristics of the nanoparticles-suspensions were deteriorated in nucleate boiling region compared with that of pure water. For the horizontal test surface, however, the CHF of the nanofluid increased 32%. These were related to the change of the heating surface characteristics by the deposition of nanoparticles on the heating surface.

You et al. (2003) carried out an experimental study on the CHF of water–Al_2O_3 nanoparticles-suspensions in a pool boiling experiment at the pressure of 20.89 kPa. The experimental results demonstrated that the CHF increased about 200% compared with pure water. However, the nucleate boiling heat transfer coefficients appeared to be the same.

On the other hand, the miniature heat pipe technology rises as a new heat transfer technology accompanied by the development of electronics, communication and computing technologies. The exponential growth of heat rejection and the miniaturization of electronic devices have brought about serious problems in the thermal management. Electronic devices normally allow the working temperature of less than 80 °C. If the temperature goes beyond this limit, the heat transfer capability of the components drops significantly and the devices may even fail to work.

Studies on the miniature flat heat pipe have been carried out. Cao et al. (1997) performed some experimental studies for several kinds of water–copper miniature flat heat pipes with micro-grooved surface. The result shows that this kind of heat pipe can enhance the heat transfer compared with the flat surface. Hopkins et al. (1999) carried out an experimental study concerning three different geometric shapes and different sizes of the copper–water miniature flat heat pipes. They concluded that the micro-grooved surface with large ratio of depth to width has better heat transfer capability than that of the flat surface.

Based on the previous researches concerning the pool boiling of nanofluids on the flat surface at atmospheric pressure, the present study focused on the experimental investigation of the nucleate boiling characteristics of nanofluids at sub-atmospheric pressure conditions. The experimental apparatus was a miniature flat heat pipe with micro-grooved surface of its evaporator.

2. Experimental apparatus and procedures

In this experiment, the deionized water was used as the base fluid. CuO nanoparticles were commercial products made by Nano Circumference Institute of Anhui Industrial University in China. The average diameter of CuO nanoparticles used in this experiment was 30 nm. The CuO nanoparticles and water were put into a super-sonic water bath and surged for about 12 h to form stable suspension. In order to prevent

the occurrence of sorption layers on the heat transfer surface formed by nanoparticles, no surfactant was added into the suspensions. Fig. 1a and b show the TEM photographs of CuO nanoparticle suspensions with the mass concentrations of 0.5 wt% and 1.0 wt%. The experimental results showed that the stability and uniformity of nanoparticle suspensions were poor after several days. However, during the test run, nanoparticle-suspensions could maintain good uniformity due to the churning effect of bubbles.

Fig. 2 shows the schematic diagram of the experimental apparatus. The apparatus mainly consisted of a test box made of stainless steel, a miniature flat heat pipe evaporator with a horizontal micro-grooved heat transfer surface on the top of the copper block, a condensing system, a data acquisition system and a power supply, a vacuum pumping unit and a liquid-filling device.

A cartridge electric heater was inserted into the cooper block from the bottom of the copper block as the main heater. The copper block was wrapped by a layer of mica film, and then the mica film was wrapped by an electrical heating ring as the auxiliary heater. The space between the copper block and the test box was filled by asbestos for insulation. The heat transfer surface and the copper baffle were sealed with silicone film. Six thermocouples having the diameter of 1 mm were inserted into copper block along the horizontal direction to measure the temperature gradient and heat flux in the upper part of the copper block as shown in Fig. 3. The vertical distance between the top thermocouple and the heat transfer surface was 4.0 mm, and the vertical distances between the thermocouples were 10.0 mm. An alarm thermocouple inserted at the bottom of the cooper bar was connected to a temperature controller for run alarming. At the top of the evaporator chamber, a thermocouple and a probe of the pressure transducer were inserted into the evaporator to measure the saturated temperature and pressure of the vapor.

Fig. 3 shows the schematic configuration of the evaporator part. The upper part of the cooper block was manufactured as a cuboid whose horizontal top surface was the heat transfer surface having a micro-grooved construction with size of 40 mm × 40 mm. The grooves were of 0.5 mm wide and 0.8 mm deep. The gap between the two grooves was 0.5 mm. Details of the grooves can be shown in Fig. 4. Six thermocouples having the diameter of 0.1 mm were inserted into copper block along the horizontal direction. The vertical distance between the top thermocouple and the micro-grooved surface was 4.0 mm and the vertical distances between the thermocouples were 10.0 mm. The size details are shown in Fig. 3. An alarm thermocouple inserted at the bottom of the cooper bar was connected to a temperature controller for run alarming. Besides, a thermocouple and a pressure transducer were inserted into the evaporator to measure the saturated temperature and the pressure of the steam. Experimental result shows that the difference between the measured saturated steam temperature and the calculated one corresponding to the measured evaporator pressure was less than 0.2 K in all runs.

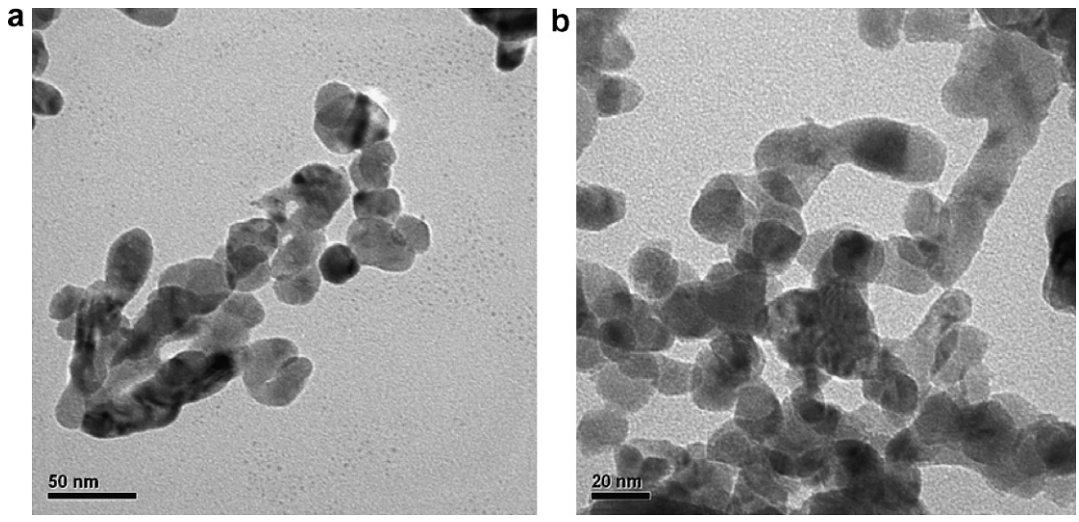

Fig. 1. TEM photographs of CuO nanoparticle suspensions. (a) Concentration of 0.5 wt% and (b) concentration of 1.0 wt%.

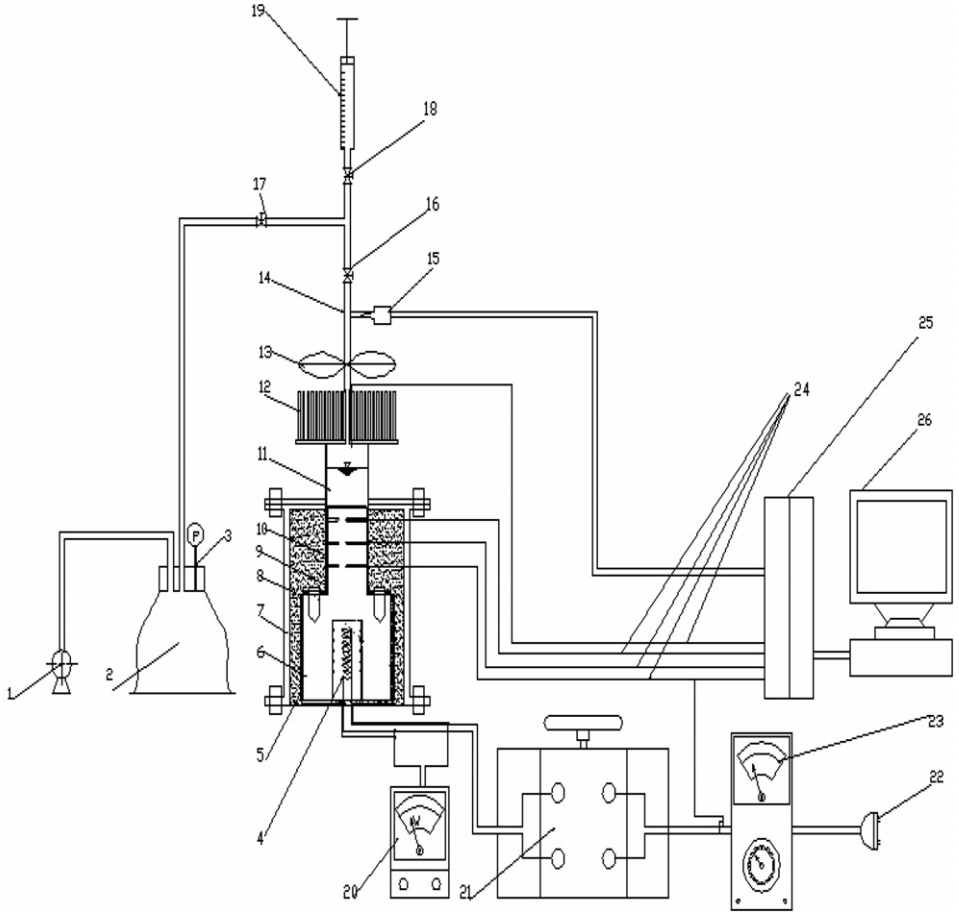

Fig. 2. Schematic diagram of experimental apparatus. 1 – Vacuum pump; 2 – glass container; 3 – pressure guage; 4 – main heater; 5 – auxiliary heater; 6 – copper block; 7 – test box; 8 – insulating material; 9 – copper baffle; 10 – sealing silicone; 11 – evaporator chamber; 12 – condenser; 13 – cooling fan; 14 – water-filled pipe; 15 – pressure transducer; 16, 17, 18 – valve; 19 – injector; 20 – wattmeter; 21 – transformer; 22 – power supply; 23 – temperature controller; 24 – thermocouples; 25 – data acquisition system; 26 – computer.

Fig. 5 shows the diagram of the liquid charging and air pumping system. According to previous researches (Cao et al., 1997; Hopkins et al., 1999), the best filling ratio ranged from 40% to 60% in which the filling ratio has no effect on the heat transfer. Therefore the filling ratio was fixed at 50% in all tests.

The test run was performed under four steady operating pressures of 100 kPa, 31.2 kPa, 20.0 kPa and 7.4 kPa (the saturated temperatures corresponding to these pressures are, respectively, 100 °C, 70 °C, 60 °C and 40 °C). In each run, the test pressure was regulated to the preset value by controlling the rotational speed of the fan. In order to reduce the heat losses from the copper block, the auxiliary heater was started to make sure that the total heating power measured by the thermocouples inside the cooper bar could be equal to that of the main heater.

In this experiment, it has been confirmed that the assumption of one-dimensional heat conduction along the vertical direction in the upper part of the copper block was well satisfied by a numerical and a test results. Therefore, the wall temperature and heat flux can be calculated according to the measured temperatures of six thermocouples. Signals from these thermocouples were measured by a data acquisition system (Agilent-34950A).

In the run, the heating power was gradually increased by an increment of 5%. When the measured wall temperature increased abruptly and could not hold a steady state, a dry-out phenomenon occurred on the wall and the electric power supply was instantly switched off. Then, the run was restarted from the former steady

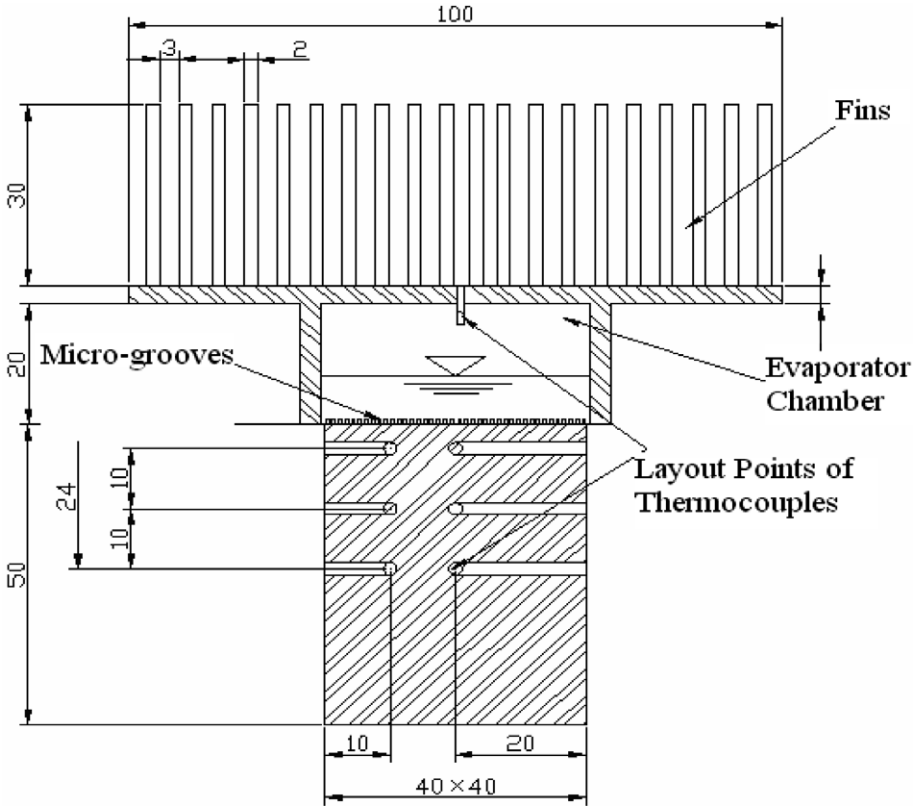

Fig. 3. Schematic configuration of evaporator (unit: mm).

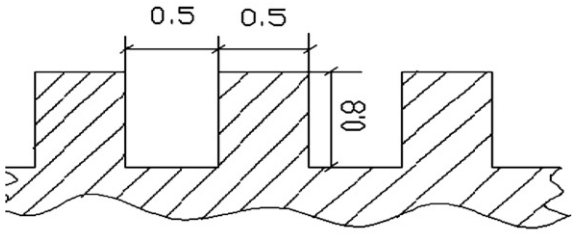

Fig. 4. Schematic diagram of the micro-groove (unit: mm).

input power and the power was increased in an increment of 1% of the former power. When the measured wall temperatures once again increased abruptly, the electric power supply was instantly switched off and the test was stopped. The CHF value was determined by the final electric power. In addition, the power supply would turn off automatically when the internal temperature of cooper bar went beyond 300 °C.

The uncertainty of the experimental data concerns five parameters as follows: (1) The maximum calibration error of the thermocouples. (2) The maximum relative location deviation between thermocouples in the vertical direction. (3) The calculated error of the thermal conductivity of the copper block. (4) The instrument errors. (5) For the measurement error of the CHF (a truncation error of the increasing step of the heating power should be added). The maximum calibration error of the thermocouple was 0.2 K. The maximum relative location deviation between thermocouples was about 1%. The calculated error of the thermal conductivity of the copper block was estimated to be 2%. The instrument error was about 0.5%. Truncation error of measurement was about 1%. Thus the maximum uncertainties of heat flux and the heat transfer coefficient were about 9% and 14%, respectively.

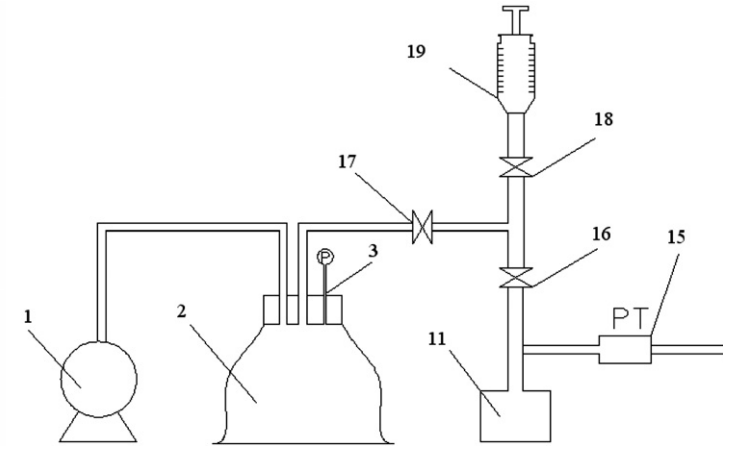

Fig. 5. The diagram of the charging and air pumping system. 1 – Vacuum pump; 2 – glass container; 3 – pressure guage; 11 – evaporator chamber; 15 – pressure transducer; 16, 17, 18 – vacuum valve and 19 – injector.

3. Experimental results and discussion

Figs. 6 and 7 show the pool boiling curves of the heat transfer coefficient, h vs. the wall heat flux, q for the deionized water under different pressure conditions using both the smooth surface and the grooved surface. The solid lines in the two figures are the calculated values according to the well-known Kutateladze correlation (Kutateladze, 1951). It can be observed that the boiling curves of water on the smooth surface were well closed to the calculated values with a maximum relative error of 27% in the nucleate boiling region.

$$\frac{h}{\lambda}\sqrt{\frac{\sigma}{g(\rho_l-\rho_v)}} = 7.0\times10^{-4}Pr_l^{0.35}\times\left[\frac{q}{\rho_v h_{fg} v_l}\sqrt{\frac{\sigma}{g(\rho_l-\rho_v)}}\right]^{0.7}\left[\frac{p}{\sigma}\sqrt{\frac{\sigma}{g(\rho_l-\rho_v)}}\right]^{0.7} \quad (1)$$

where σ is the liquid–gas interface tension, ρ_l and ρ_g the liquid and gas density, v_l the kinematical viscosity of the liquid, p the pressure, g the gravity acceleration, λ the thermal conductivity of fluid, h_{fg} the latent heat of evaporation, Pr_l the Prandtl number of saturated liquid.

It can be observed from Fig. 7 that there was a significant heat transfer enhancement caused by the micro-grooved surface at atmospheric pressure. The increase of the heat transfer coefficient ranged from 40% to 50%. However, there was no obvious heat transfer enhancement at sub-atmospheric conditions.

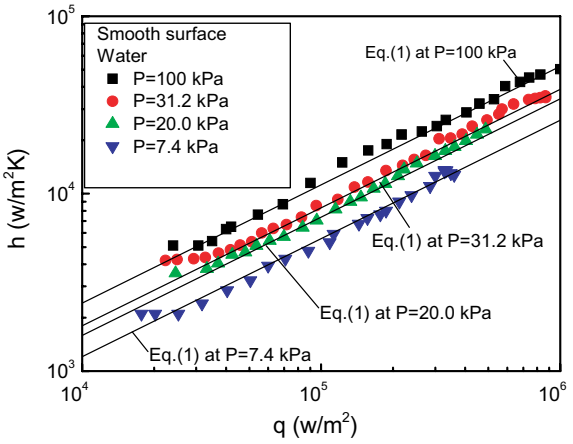

Fig. 6. Boiling heat transfer of water at different pressures on smooth surface.

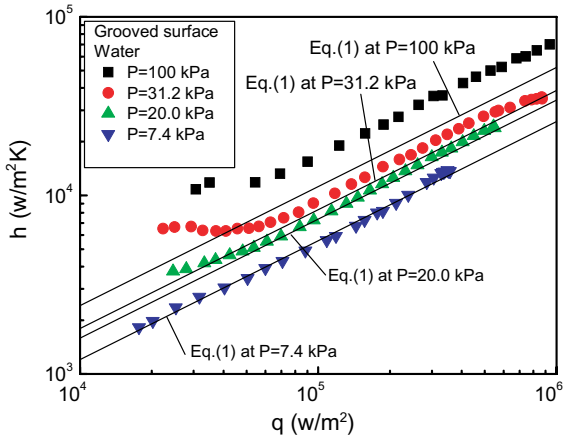

Fig. 7. Boiling heat transfer of water at different pressures on grooved surface.

Fig. 8a–c show the boiling curves of the heat transfer coefficient vs. the heat flux for the nanofluids at different mass concentrations ranging from 0.1 wt% to 2.0 wt%. The operating pressures are 100 kPa, 20.0 kPa and 7.4 kPa, respectively. The mass concentration of nanofluids, ω has great influence on the nucleate boiling heat transfer for all pressures. At each pressure, the heat transfer coefficients of nanofluids are gradually enhanced with the increase of the mass concentration when the concentration is less than 1.0 wt%. The maximum enhancement corresponds to the concentration of 1.0 wt% and the heat transfer coefficient of nanofluids can be doubled at sub-atmospheric pressures compared with that of the water. However, when the concentration is over 1.0 wt%, the heat transfer coefficients show a slight worsening trend. Therefore there exists an optimum mass concentration for nanofluids which corresponds to the maximum heat transfer enhancement. This optimum mass concentration is 1.0 wt% at all pressures. Comparing with those of water, the heat transfer coefficients of nanofluids can maximally increase about 25%, 100% and 150% under atmospheric pressure, 20.0 kPa and 7.4 kPa pressures, respectively.

To investigate the effect of the heat transfer surface state on the boiling characteristics of nanofluids, Fig. 9 illustrates the comparison of the boiling heat transfer of the nanofluid with 1.0 wt% concentration for the smooth surface and the grooved surface. It is found that the boiling heat transfer of the nanofluid on the smooth surface is almost the same with that of water on the smooth surface at atmospheric pressure. Meantime, boiling heat transfer of the nanofluids on the grooved surface increases remarkably compared with that on the smooth surface at atmospheric pressure. Therefore, the grooved surface can significantly enhance the heat transfer of the nanofluids at atmospheric pressure. For sub-atmospheric pressures, the boiling heat transfer of the nanofluid on the smooth surface is close to that on the grooved surface. The grooved surface has negligible impact on the heat transfer of the nanofluids at the sub-atmospheric pressure.

The effect of the pressure on the boiling heat transfer enhancements of nanofluids is shown in Fig. 10. Here, h denotes the heat transfer coefficient of nanofluid while h_0 that of water. It is found that the boiling heat transfer enhancement of the of nanofluids increase greatly with the decrease of the test pressure. At atmospheric pressure, the maximum enhancement is about 25% compared with that of water. However, the heat transfer coefficient can increase about 100% at the pressure of 20.8 kPa and about 150% at the pressure of 7.4 kPa, as compared with that of water. Besides, the experimental results also show that the heat transfer of nanofluids can be strengthened with the increase of the heat flux.

Fig. 11 shows the influence of nanofluids concentration on the CHF enhancement ratio. Here, q_c is the CHF of the nanofluids at different concentrations and $q_{c,0}$ the CHF of water. The experimental results show that the CHF enhancement ratio first increases with the increase of the nanoparticles mass concentration and it gradually trends to a constant value when the nanoparticles concentration is over 1.0 wt%. At atmospheric pressure, the CHF of nanofluids can increase 50% compared with that of water and it increases 200% at the pressure of 7.4 kPa. The enhancement effect is more significant at sub-atmospheric pressures than that at atmospheric pressure.

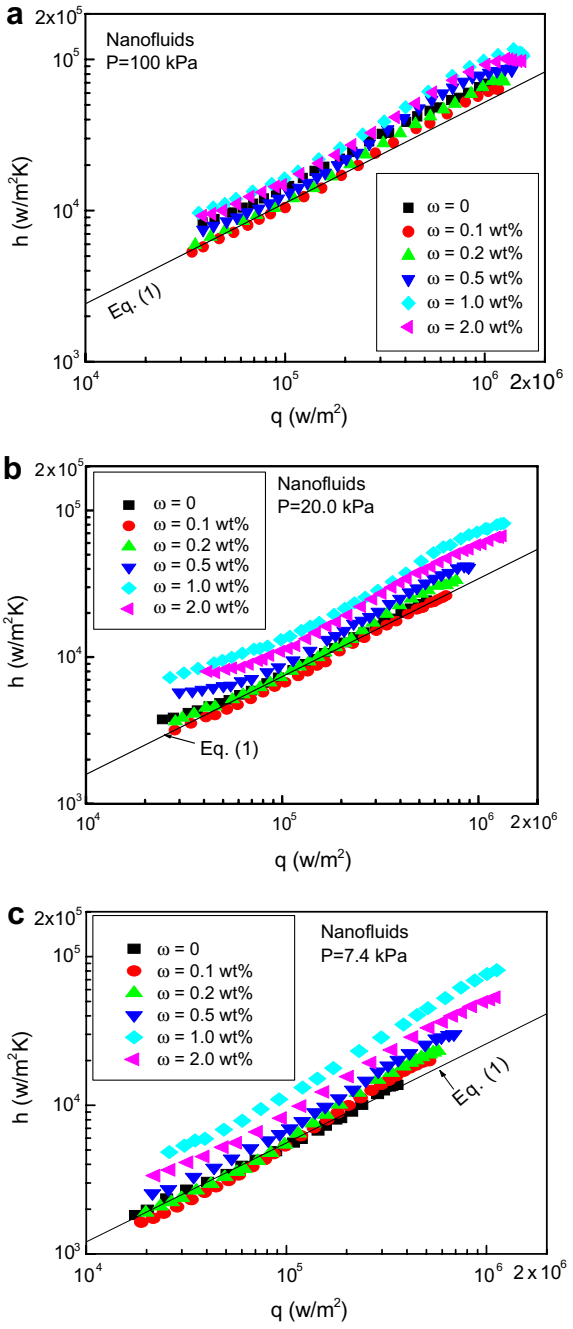

Fig. 8. Boiling heat transfer of nanofluids under different pressures on grooved surface. (a) $p = 100$ kPa; (b) $p = 20.0$ kPa and (c) $p = 7.4$ kPa.

After the boiling tests, the test surface was cut as a small square specimen and cleaned by water jet. Then, the microphotographs of the heat transfer surface were taken. After the test using water, the surface was smooth and had a metallic brilliancy. The surface was slightly oxidized. However, for the surface after the test using CuO nanoparticles suspension, there was a thin coating layer formed on the surface. Fig. 12 shows the 2-D and 3-D atomic force microscope (Nanoscope IIIa) microphotographs. The surface was covered by a very thin, smooth, block coating layer, which should be formed by the nanoparticles trapped in the cavities on the

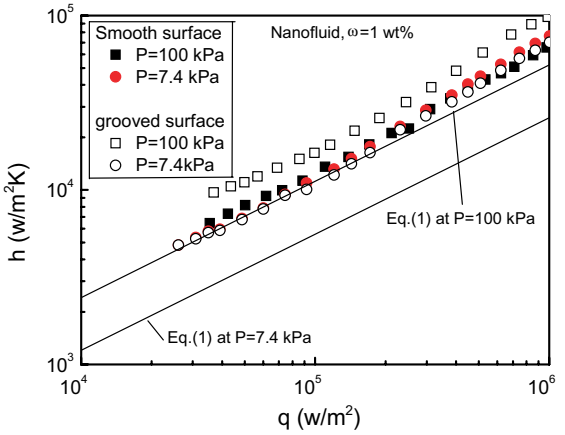

Fig. 9. Comparison of boiling heat transfer of nanofluids for smooth and grooved surfaces.

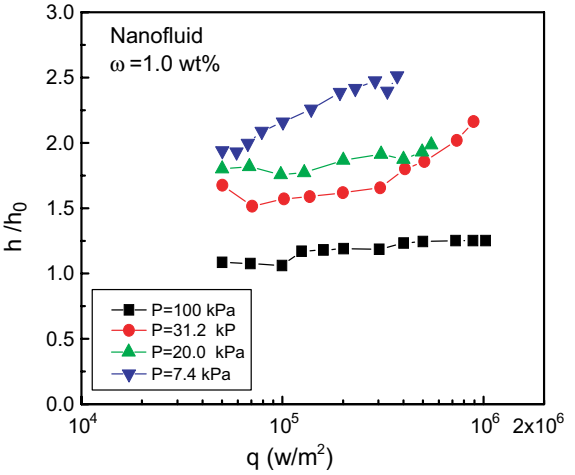

Fig. 10. Effects of pressures on the heat transfer enhancement for nanofluid with concentration of 1.0 wt%.

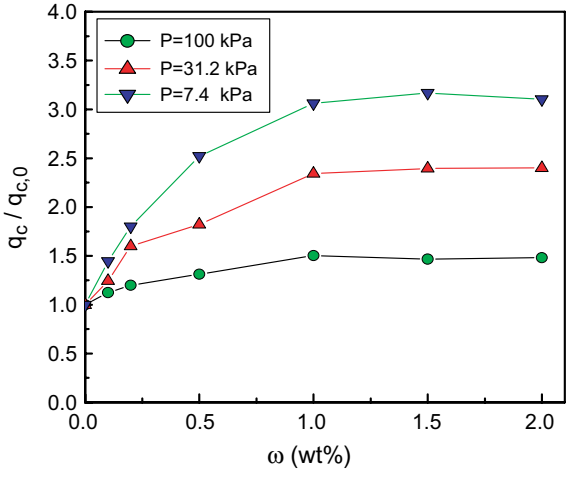

Fig. 11. Effect of concentration of nanofluids on CHF enhancement at different pressures.

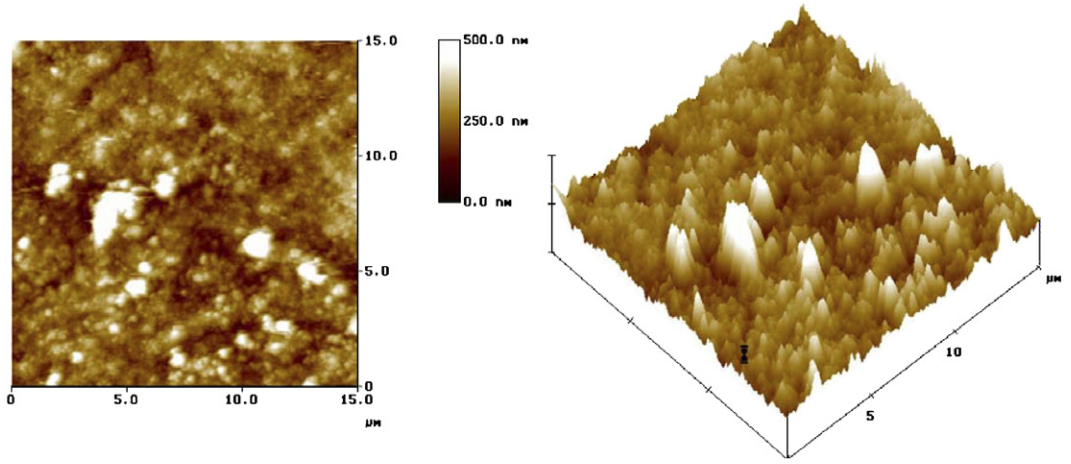

Fig. 12. 2-D and 3-D microphotographs of the surface status after CuO nanofluid test and cleaning process.

copper surface. Therefore, a very thin coating layer of nanoparticles would bond on the copper surface after boiling experiment using the nanoparticles-suspensions.

Previously the boiling experimental study of nanofluids concentrated almost on pool boiling on a smooth surface at atmospheric pressure conditions. In these experiments, the boiling heat transfer was for the worse or no change and the CHF had some increase (20–40%) compared with those of the based liquids. Das et al. (2003b) reported that a reduction in the surface roughness had taken place after the boiling test using nano-suspensions. Since the size of the nanoparticles are one to two orders of magnitude smaller than the roughness of the copper surface, the particles sit on relatively uneven surface and formed a coating layer during boiling. They guessed that the decrease of the surface roughness reduces the boiling heat transfer of the nanoparticles suspensions. On the other hand, Bang and Chang (2005) guessed that the CHF is mainly affected by the various surface characteristics, such as the solid–liquid contact angle. The CHF would increase with decrease of the solid–liquid contact angle due to the formation of the coating layer on the heat transfer surface (Kandlikar, 2001).

In the present study, the experimental results from the atmospheric pressure condition agree basically with the other researcher's work mentioned above. However, the heat transfer coefficients and the CHFs of the nanofluids boiling at low pressure conditions have a dramatic increase. It is unclear that why the test pressure has so great influence on the heat transfer enhancement of the nanofluids.

In the present stage, two traditional heat transfer theory concerning the pool boiling enhancement of nanofluids may be proposed to explain the mechanism of the boiling heat transfer of the nanofluids. One is the change of the fluid physical properties and the other is the change of the heat transfer surface characteristics. The effect of the fluid physical properties on the heat transfer can be observed from Eq. (1). In the present study, the values of thermal conductivity, viscosity, and the surface tension of nanofluids were measured. They are 102%, 101% and 88% of those of water at the condition of atmospheric pressure, room temperature and the mass concentration of 1.0 wt%. Changes of these properties can be neglected at different pressures and temperatures. Therefore, by Eq. (1), the heat transfer coefficient of nanofluids should have slight decrease compared with that of water. The effect of the heat transfer surface characteristics on the boiling heat transfer is very complex. Since the size of the nanoparticles is one to two orders of magnitude smaller than the particles of the copper surface, the depositing of the nanoparticles unevens the surface and forms a coating layer during boiling. Therefore, both the surface roughness and the solid–liquid contact angle would decrease. The boiling heat transfer coefficient of nanofluids would decrease and the CHF would increase. This mechanism can explain some of the experimental results at atmospheric pressure reported by previous researchers. However, if the heat transfer surface was covered by a large number of the aggregated particles and a porous layer was formed on the surface, then, the both of boiling heat transfer coefficient and CHF would obtain significant increase. This mechanism can give reason for the present experimental results under sub-atmospheric

pressures. It is guessed that this porous layer formed from aggregated particles can only steady exist at sub-atmospheric pressure, and the forming, growing up and departing of bubbles of nanofluids at sub-atmospheric pressures may have great change compared those at atmospheric pressure.

Repeating tests were also carried out to find out the difference of heat transfer characteristics between the fresh nanofluids and the old nanofluids. After the tests using fresh nanofluids, the test system was left standing for two weeks. Then the run was restarted. The repeating tests indicate that no meaningful differences of the heat transfer characteristics were found between the fresh and the old nanofluids. The reason should be due to the stirring effect of the bubbles for the suspension during boiling process. For the old nanofluid in the evaporator, the aggregated nanoparticles depositing on the heating surface could quickly spread into the base liquid and can form a uniform suspension again under the effect of the buoyant force and boiling bubbles when the run was reheated.

Summing the mentions above, it is confirmed that water–CuO nanoparticle suspension can significantly strengthen the boiling heat transfer coefficient and the heat transfer capacity of the MFHP with micro-grooved surface under sub-atmospheric conditions. Nanofluid is a potential working fluid to enhance the heat transfer characteristics of the heat pipe.

4. Conclusion

1. At atmospheric pressure, the micro-grooved heat transfer surface can enhance the boiling heat transfer characteristics of water as compared with that on smooth surface. However, at low pressure, the heat transfer enhancement effect of the grooved surface almost disappears.
2. The mass concentration of nanofluids has remarkable influence on the both of boiling heat transfer coefficient and CHF of the nanofluids. The heat transfer coefficient and the CHF increase with the increase of the concentration when the mass concentration is less than 1%. However, when the concentration is over 1 wt%, the CHF is basically close to a constant value, and the heat transfer deteriorates gradually. There exists an optimum mass concentration for nanofluids which corresponds the maximum heat transfer enhancement and this optimum mass concentration is 1% at all test pressures.
3. The pressure has very significant influence on the both of boiling heat transfer enhancement and CHF enhancement of nanofluids, the heat transfer coefficient and the CHF of nanofluids greatly increase with the decrease of the test pressure. At atmospheric pressure, the heat transfer coefficient and the CHF can increase, respectively, about 25% and 50%, and they can increase about 150% and 200% at the pressure of 7.4 kPa.
4. CuO nanoparticles suspension as a working fluid can significantly strengthen the heat transfer performance and the maximum power of the miniature flat heat pipe evaporator with micro-grooved surface under low pressure conditions. Nanofluid is a potential new kind of working fluid to enhance the heat transfer characteristics of heat pipe.

Acknowledgement

This study was supported by Key basic research program of Science and Technology Bureau of Shanghai under Grant No. 04JC14049.

References

Bang, I.C., Chang, S.H., 2005. Boiling heat transfer performance and phenomena of Al_2O_3–water nanofluids from a plain surface in a pool. Int. J. Heat Mass Transfer 48, 2407–2419.

Cao, Y., Gao, M., Beam, J.E., 1997. Experiments and analyses of flat miniature heat pipes. J. Thermophys. Heat Transfer 11, 158–164.

Das, S.K., Putra, N., Roetzel, W., 2003a. Temperature dependence of thermal conductivity enhancement for nanofluids. J. Heat Transfer 125, 567–574.

Das, S.K., Putra, N., Thlesen, P., Roetzel, W., 2003b. Pool boiling characteristics of nanofluids. Int. J. Heat Mass Transfer 46, 851–862.

Eastman, J.A., Choi, S.U.S., Li, S., Yu, W., Thmpson, L.J., 2001. Anomalously increasing effective thermal conductivities of ethylene glycol-based nanofluids containing copper nanoparticles. Appl. Phys. Lett. 78, 718–720.

Hopkins, R., Faghri, A., Knustalev, D., 1999. Flat miniature heat pipes with micro capillary grooved surface. J. Heat Transfer 12, 102–109.

Kandlikar, S.G., 2001. A theoretical model to predict pool boiling CHF incorporating effects of contact angle and orientation. J. Heat Transfer 123, 1071–1079.

Kutateladze, S.S., 1951. A hydrodynamic theory of changes in the boiling process under free convection conditions. Isv. Akad. Nauk, USSR, Otd. Tekh. Nauk 4, 529–935.

Lee, S., Chois, S.U.S., Li, S., Eastman, J.A., 1999. Measuring thermal conductivity of fluids containing oxide nanofluids. J. Heat Transfer 121, 280–289.

Maiga, S.E.B., Nguyen, C.T., Galanis, N., Roy, G., 2004. Heat Transfer behaviors of nanofluids in a uniformly heated tube. Superlattice. Microstruct 26, 543–557.

Vassallo, P., Kuman, R., Amico, S.D., 2004. Pool boiling heat transfer experiments in silica–water nano-fluids. Int. J. Heat Mass Transfer 47, 407–411.

Wang, B.X., Zhou, L.P., Peng, X.P., 2003. A fractal model for predicting the effective thermal conductivity of liquid with suspension of nanoparticles. Int. J. Heat Mass Transfer 46, 2665–2672.

Wen, D.S., Ding, Y.L., 2004. Effective thermal conductivity of aqueous suspensions of carbon nanotubes (nanofluids). J. Thermophys. Heat Transfer 18, 481–485.

Wen, D.S., Ding, Y.L., 2005. Experimental investigation into the pool boiling heat transfer of aqueous based alumina nanofluids. J. Nanoparticles Res. 7, 265–275.

Xuan, Y.M., Li, Q., 2003. Investigation on convective heat transfer and flow features of nanofluids. J. Heat Transfer 125, 151–155.

You, S.M., Kim, J.H., Kim, K.H., 2003. Effect of nanoparticles on critical heat flux of water in pool boiling heat transfer. Appl. Phys. Lett. 83, 3374–3376.